Third AO4ELT Conference - Adaptive Optics for Extremely Large Telescopes
Florence, Italy. May 2013
ISBN: 978-88-908876-0-4
DOI: 10.12839/AO4ELT3.13326

C_N^2 PROFILE RECONSTRUCTION WITH SHACK-HARTMANN SLOPE AND SCINTILLATION DATA: FIRST ON-SKY RESULTS

Juliette Voyez[1a], Clélia Robert[1], Jean-Marc Conan[1], Laurent Mugnier[1], Vincent Michau[1], Bruno Fleury[1], Etienne Samain[2], and Aziz Ziad[3]

[1] ONERA, The French Aerospace Lab, Châtillon, France
[2] Laboratoire Géoazur, Université de Nice-Sophia Antipolis, CNRS, OCA, Caussols, France
[3] Laboratoire Lagrange, Université de Nice-Sophia Antipolis, CNRS, OCA, Nice, France

Abstract. All Wide Field Adaptive Optics (WFAO) systems for the ELTs need a precise tomographic reconstruction of the turbulent volume. The C_n^2 profile, representing the turbulence strength, becomes a critical parameter to predict and improve WFAO system performance. CO-SLIDAR (COupled SLope and scIntillation Detection And Ranging) is a method using both correlations of slopes and correlations of scintillation measured with a Shack-Hartmann (SH) on a binary star. CO-SLIDAR leads to a precise retrieval of the C_n^2 profile for both low and high altitude layers. We present the first on-sky results of the method. A SH with 30×30 subapertures is set up on a 1.5 m telescope. Images are recorded on a binary star. Preliminary data reductions are performed to check the hypothesis of Kolmogorov turbulence. We also control the hypothesis of weak perturbation regime. We finally estimate the C_n^2 profiles. The results are compared with those of methods which are only using correlations of slopes or of scintillation. We discuss the contribution of the CO-SLIDAR as a new C_n^2 profiler.

1 Introduction

The vertical distribution of turbulence strength, known as the C_n^2 profile, is a key-point in the development of next-generation AO systems. A good knowledge of the C_n^2 profile is necessary for site characterization and WFAO system design. High-resolution profiles would help WFAO system optimisation [1,2], and are needed to perform accurate simulations of WFAO systems so as to predict their performance [3]. Moreover, the C_n^2 profile is a parameter of great importance in the case of AO-corrected image deconvolution with a variable point spread function in the field of view [4–6]. An accurate knowledge of the C_n^2 profile could also support optical turbulence forecast [7].

SLODAR (SLOpe Detection And Ranging) [8,9] uses correlations of slopes measured on a binary star with a SH to estimate the turbulent profile. Other methods take benefit of correlations of scintillation, such as G-SCIDAR (Generalized-SCIntillation Detection And Ranging) [10, 11], also working on a binary star, and MASS (Multiple Aperture Scintillation Sensor) [12], which uses the correlations of scintillation measured on a single star.

CO-SLIDAR [13] is a new C_n^2 profiler, combining sensitivity to both low and high altitude layers, which jointly uses correlations of slopes and of scintillation, both measured on a binary star with a SH. CO-SLIDAR's first validation in simulation have been presented in [13]. The next step is a full experimental validation of the concept.

[a] juliette.voyez@onera.fr

This paper presents the very first on-sky results of the CO-SLIDAR C_n^2 profiler. A more detailed analysis will be presented in [14]. CO-SLIDAR is tested on-sky on the 1.5 m MeO telescope. Images on a binary star are acquired to extract slope and scintillation data. Their correlations are computed so as to estimate C_n^2 profiles. Results are compared to those obtained from correlations of slopes only or of scintillation only. We finally discuss the CO-SLIDAR contribution in the C_n^2 profilers' landscape.

This paper is organized as follows. In section 2 we recall CO-SLIDAR theoretical background. In section 3 we present the experiment and detail data analysis. Section 4 is dedicated to experimental results. In section 5 we discuss the contribution of the CO-SLIDAR as a new C_n^2 profiler. Our conclusions are given in section 6.

2 CO-SLIDAR theoretical background

2.1 CO-SLIDAR principle

Given a double star with angular separation $\boldsymbol{\theta}$ in the field of view, the SH data at a given time t are a set of wavefront slopes and scintillation indices per star.

For a star at angular position $\boldsymbol{\alpha}$ and a subaperture with horizontal u and vertical v coordinates in the SH array, the slope measured in subaperture (u, v), denoted $\mathbf{s}_{u,v}(\boldsymbol{\alpha})$, is a bidimensional vector with components $s^k_{u,v}$ along the k-axis, $k \in \{x, y\}$. The star intensity in subaperture (u, v), $i_{u,v}(\boldsymbol{\alpha})$, leads to the scintillation index $\delta i_{u,v}(\boldsymbol{\alpha}) = \frac{i_{u,v}(\boldsymbol{\alpha}) - \langle i_{u,v}(\boldsymbol{\alpha})\rangle}{\langle i_{u,v}(\boldsymbol{\alpha})\rangle}$ where $\langle i_{u,v}(\boldsymbol{\alpha})\rangle$ is the temporal average of $i_{u,v}(\boldsymbol{\alpha})$.

Spatial correlations of slopes $\langle s^k_{u,v} s^l_{u+\delta u,v+\delta v}\rangle(\boldsymbol{\theta})$ and spatial correlations of scintillation indices $\langle \delta i_{u,v} \delta i_{u+\delta u,v+\delta v}\rangle(\boldsymbol{\theta})$, calculated between subapertures (u, v) and $(u + \delta u, v + \delta v)$, of separation vector $\boldsymbol{\rho} = (\delta u, \delta v)$, are directly related to integrals of the $C_n^2(h)$ weighted by theoretical functions W^{kl}_{ss} and W_{ii}.

In CO-SLIDAR, we compute both cross-correlations, combining the measurements on the two stars, and auto-correlations, corresponding to the measurements on a single star. Correlations of slopes bring sensitivity to ground and low altitude layers, whereas correlations of scintillation mainly give sensitivity to high altitude layers.

2.2 Direct problem

In CO-SLIDAR, we exploit only correlations of x-slopes, of y-slopes and of scintillation. Correlations are averaged over all pairs of subapertures with given separation and represented as auto- and cross-correlation maps. Then, one pixel of these maps represents the pseudo-measurement that can be written, respectively for correlations of slopes and of scintillation, as:

$$C^{kk}_{ss}(\delta u, \delta v, \boldsymbol{\theta}) = \frac{\sum_{u,v} \langle s^k_{u,v} s^k_{u+\delta u,v+\delta v}\rangle(\boldsymbol{\theta})}{N(\delta u, \delta v)}, \tag{1}$$

$$C_{ii}(\delta u, \delta v, \boldsymbol{\theta}) = \frac{\sum_{u,v} \langle \delta i_{u,v} \delta i_{u+\delta u,v+\delta v}\rangle(\boldsymbol{\theta})}{N(\delta u, \delta v)}. \tag{2}$$

$\sum_{u,v}$ denotes the summation over all overlapping subapertures and $N(\delta u, \delta v)$ represents the number of pairs of subapertures with separation $\boldsymbol{\rho} = (\delta u, \delta v)$. The pseudo-measurements given by

equations (1) and (2) are then stacked into a single vector $\mathbf{C_{mes}}$, related to the discretized C_n^2 profile at different altitudes $\mathbf{C_n^2}$, by the following linear relationship:

$$\mathbf{C_{mes}} = M\mathbf{C_n^2} + \mathbf{C_d} + \mathbf{u}. \tag{3}$$

M is the matrix of the weighting functions W_{ss}^{kk} and W_{ii}. Slope and scintillation data are affected by detection noises and the pseudo-measurements $\mathbf{C_{mes}}$ are biased with their averaged correlations $\mathbf{C_d}$. As we estimate the correlations from a finite number of frames, $\mathbf{u}$ represents a convergence noise, which we assume to be Gaussian in the following.

2.3 Problem inversion

The C_n^2 profile is retrieved minimizing the following maximum likelihood (ML) criterion, under positivity constraint:

$$J_{\mathrm{ML}}\left(\mathbf{C_n^2}\right) = \left(\mathbf{C_{mes}} - \mathbf{C_d} - M\mathbf{C_n^2}\right)^{\mathrm{T}} C_{\mathrm{conv}}^{-1}\left(\mathbf{C_{mes}} - \mathbf{C_d} - M\mathbf{C_n^2}\right). \tag{4}$$

As the C_n^2 is always positive, we minimize J_{ML} under positivity constraint. $C_{\mathrm{conv}} = \langle \mathbf{u}\mathbf{u}^{\mathrm{T}} \rangle$ is the covariance matrix of $\mathbf{u}$.

Assuming that the noises are not correlated between the two directions of observation and between different subapertures, only the variances of slopes and of scintillation are biased. These variances are averaged over all subapertures and represent the central point of the auto-correlation maps. Three new parameters, *i.e.* the variances of the noises on x-slopes, y-slopes and scintillation indices, are estimated jointly with the C_n^2 profile, without changing the ML criterion given by equation (4).

We can also minimize a metric composed of the ML criterion J_{ML} and a regularization metric designed to enforce smoothness of the C_n^2 profile. In this paper, we choose a gradient regularization. The resulting maximum *a posteriori* (MAP) criterion is:

$$J_{\mathrm{MAP}}\left(\mathbf{C_n^2}\right) = \left(\mathbf{C_{mes}} - \mathbf{C_d} - M\mathbf{C_n^2}\right)^{\mathrm{T}} C_{\mathrm{conv}}^{-1}\left(\mathbf{C_{mes}} - \mathbf{C_d} - M\mathbf{C_n^2}\right) + \beta \| \left(\nabla \mathbf{C_n^2}\right) \|^2. \tag{5}$$

3 Experiment and data analysis

3.1 CO-SLIDAR instrument

The experiment took place on the Plateau de Calern, at the Observatoire de la Côte d'Azur, near Nice, in South of France. We used the 1.5 m MeO telescope, with a central obscuration of 30 %, coupled to a 30×30 subaperture SH, hence the subaperture diameter is $d_{\mathrm{sub}} = 5$ cm. The observation wavelength was $\lambda = 517$ nm, with $\Delta\lambda = 96$ nm. The camera used was an Andor-iXon3-885 electron multiplication CCD (EMCCD) with a quantum efficiency of about 50 %, and a detector read-out noise close to one e^-/pixel.

3.2 Observations

Observations were done on May 2012, on the binary star Mizar AB. We selected the data from May, 15^{th}, around $01:00$ UT. The zenith angle of the binary star was $\zeta = 35^o$. The exposure time was $t_{\mathrm{exp}} = 3$ ms, to freeze the turbulence. The separation between the two components is $\theta = 14.4$" and their visible magnitudes are 2.23 and 3.88, leading to about 260 and 60 photons per subaperture and per frame. We recorded sequences of 1000 images at 15 Hz, so the sequence duration is about 1 min. Typical on-sky images are shown in figure 1.

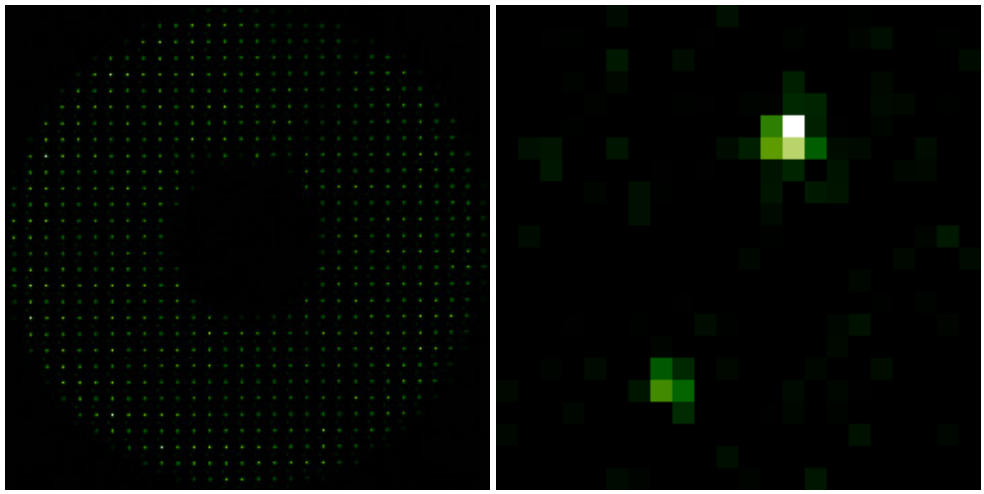

Fig. 1. SH experimental turbulent images, for a 3 ms exposure time. Left: full SH long exposure image. Right: subaperture short exposure image. Images were acquired around 01 : 00 UT, on May 15^{th}, 2012

3.3 Data analysis

We extract slopes and scintillation indices from these images. Slopes are measured using a center of gravity (COG) algorithm, in windows of 9×9 pixels, centered on the maximum of each star. The intensities, from which we deduce the scintillation indices, correspond to the sum of all pixel intensities included in the windows. From slopes we compute the Zernike coefficient variances, presented in figure 2. We reconstruct 15 radial orders. The Fried parameter r_0 is estimated excluding orders 1 and 2. We compare the experimental variances with the Noll variances and the theoretical variances with outer scale effect. We assume that $L_0 = 27$ m, which is the median outer scale observed at the Plateau de Calern [15]. We find good agreement with Kolmogorov turbulence, with outer scale effect. We check the hypothesis of weak perturbation

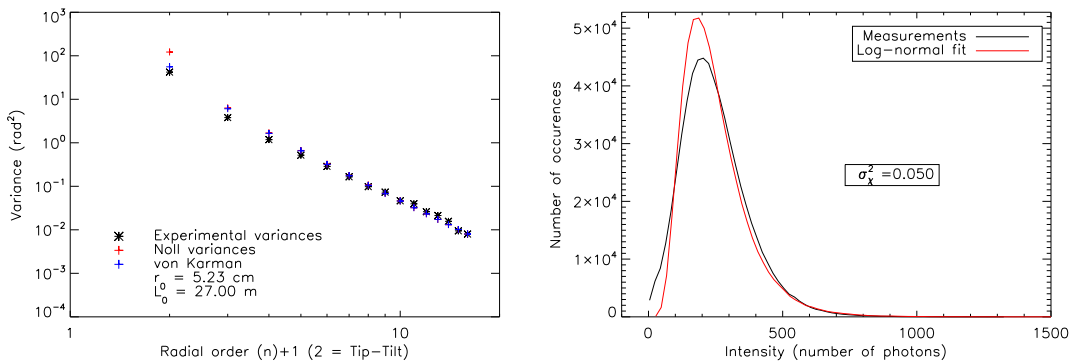

Fig. 2. Left: experimental variances of Zernike coefficients and comparison with Noll variances and von Kármán variances. Right: intensity distribution and comparison with a log-normal distribution. Data were acquired around 01 : 00 UT, on May 15^{th}, 2012, with a 3 ms exposure time.

regime using intensities and scintillation indices, by fitting a log-normal distribution. The result is presented in figure 2. The intensity distribution is very close to the expected log-normal distribution and $\sigma_\chi^2 < 0.3$ so we are in the weak perturbation regime.

4 Experimental results

4.1 Correlation maps

The correlation maps are presented in figure 3. The auto-correlation maps have a maximum at their center. They represent the response of the system to the integral of turbulence. The cross-correlation map of scintillation shows peaks of correlation in the top right quarter of the map, in the alignment direction of the stars, representing the turbulent layers' signatures. In the cross-correlation maps of slopes, only the peak of correlation corresponding to $h = 0$ is visible, at the center of the map. The peaks of correlation associated to the other layers are also located at $\boldsymbol{\theta} h$, but because of the width of the response and its decreasing strength with altitude, they are not visible to the naked eye. In CO-SLIDAR, we use both slope and scintillation responses to be sensitive to low and high altitude turbulent layers.

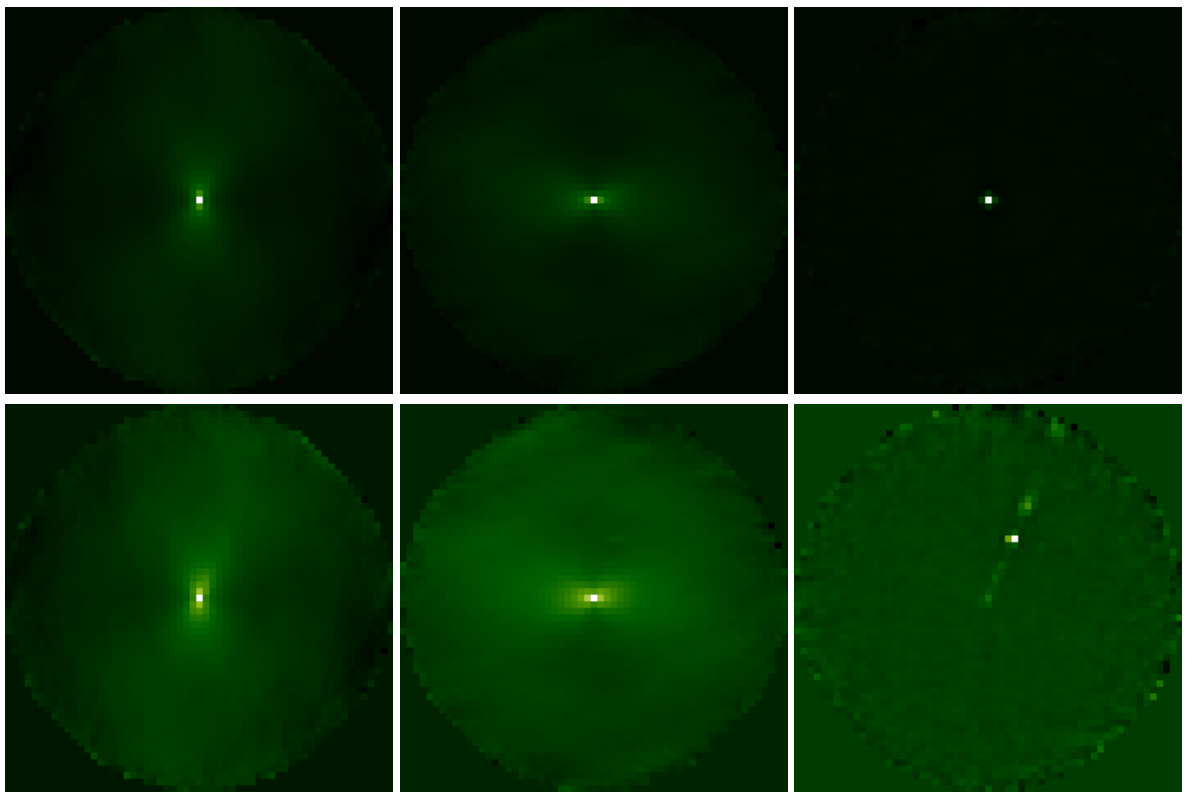

Fig. 3. Correlation maps from experimental slope and scintillation data. Top: auto-correlation maps, bottom: cross-correlation maps. Left: correlations of x-slopes, middle: correlations of y-slopes, right: correlations of scintillation. Data from May 15^{th}, 2012, around $01:00$ UT.

4.2 Reconstruction of the C_n^2 profiles

As we use a von Kármán model for turbulence, we have to choose an outer scale L_0. We assume that $L_0 = 27$ m. We checked that the results are not significantly affected by the outer scale choice in the range $[10\,;50]$ m. We estimate 30 layers. The altitude resolution is $\delta h \simeq \frac{d_{\text{sub}}}{\theta} \cos\zeta \simeq$ 600 m and the maximum altitude of sensitivity is $H_{\max} \simeq \frac{D}{\theta} \cos\zeta \simeq 17$ km.

The C_n^2 profiles are estimated with the ML solution, from correlations of slopes only, of scintillation only and with the CO-SLIDAR method. The results are presented in figure 4. We

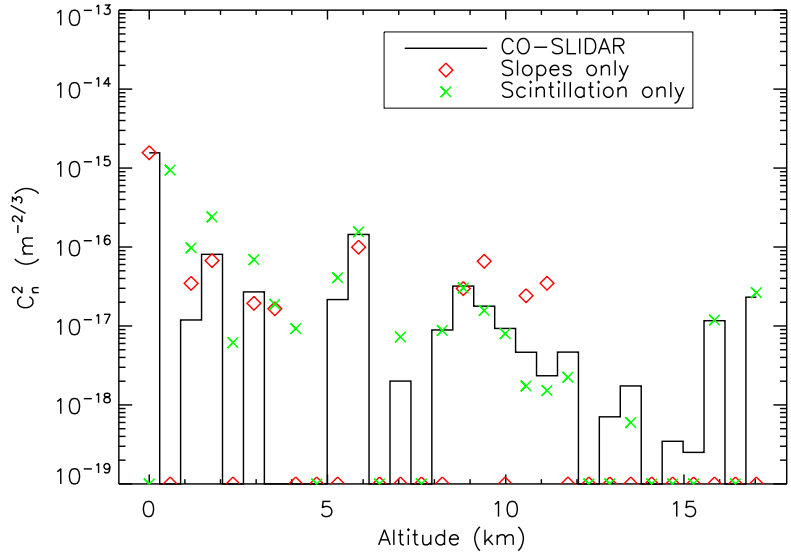

Fig. 4. ML reconstruction of the C_n^2 profile from correlations of slopes only, of scintillation only and with the CO-SLIDAR method. Data from May 15^{th}, 2012, around 01 : 00 UT.

see a good agreement between the CO-SLIDAR reconstruction and the estimation from correlations of slopes at low altitude, but at medium altitude, the latter overestimates the turbulence. The estimation from correlations of scintillation alone is more questionable. We observe a good agreement with the CO-SLIDAR reconstruction at high altitude, but at low altitude, the turbulence is strongly over-estimated, compared to the CO-SLIDAR estimation.

Then we estimate the C_n^2 profile with the MAP solution. The corresponding C_n^2 profile is shown in figure 5, and compared to the one without regularization. We get a smoother profile, slightly different from the ML one, because less layers are estimated to zero.

The CO-SLIDAR profiles show strong turbulence at low altitude, another strong layer around 5 km, and some weaker layers in altitude. This shape of turbulence profile is typical of an astronomical site. The CO-SLIDAR method, with this instrument's geometry, allows to estimate the C_n^2 profile from the ground to 17 km, with a resolution of 600 m.

5 CO-SLIDAR in the C_n^2 profilers' landscape

The results presented in the previous section confirm that CO-SLIDAR on meter class telescopes provides high resolution C_n^2 profiles. This new method could be used for site characterization to obtain relevant inputs for WFAO design and performance evaluation, or to help optical turbulence forecast.

The joint use of correlations of slopes and of scintillation leads to a more robust profile estimation, with better resolution over the whole altitude range. Of course, inter-comparisons

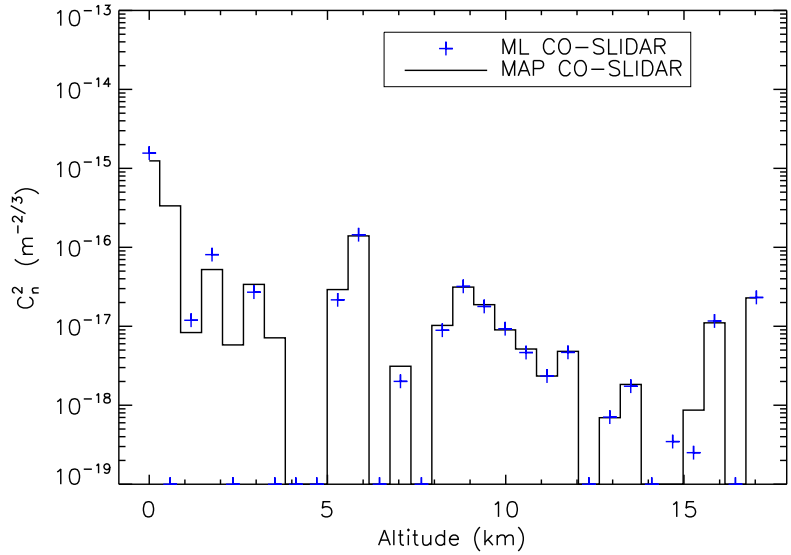

Fig. 5. CO-SLIDAR ML and MAP reconstructions of the C_n^2 profile. Data from May 15^{th}, 2012, around 01 : 00 UT.

are needed, with the reference profilers SLODAR, G-SCIDAR and MASS, and with new-generation profilers, such as PBL (Profileur Bord Lunaire) [16] and Stereo-SCIDAR [17]. A multi-instrument campaign dedicated to this comparison is foreseen [18].

WFAO systems will include several wavefront sensors, leading to multi-directional SLODARs [19,20], but external high resolution C_n^2 profiles are also needed for the calibration of these systems.

6 Conclusion

We have presented the first-on sky results of the CO-SLIDAR C_n^2 profiler. C_n^2 profiles have been estimated from both correlations of slopes and of scintillation. We plan a comparison with free atmosphere C_n^2 profiles deduced from meteorological data. This work will be presented in a forthcoming paper [14]. Other observation campaigns are needed to calibrate and compare CO-SLIDAR with other C_n^2 profilers.

Aknowledgements

This work has been performed in the framework of a Ph.D Thesis supported by Onera, the French Aerospace Lab, and the French Direction Générale de l'Armement (DGA). The authors are very grateful to the team operating at MeO station, for the use of the 1.5 m telescope and their help and support throughout the whole campaign. The authors also want to thank F. Mendez for his help in optomechanics.

References

1. M. Le Louarn, N. Hubin, M. Sarazin, and A. Tokovinin. Mon. Not. R. Astron. Soc., **317**, 2000, 535–544.

2. T. Fusco, J. M. Conan, G. Rousset, L. Mugnier, and V. Michau. J. Opt. Soc. Am. A, **18**, 2001, 2527–2538.
3. A. Costille and T. Fusco. In *2nd AO4ELT Conference*, Victoria, 2011.
4. T. Fusco, J. M. Conan, L. M. Mugnier, V. Michau, and G. Rousset. Astron. Astrophys. Suppl. Ser., **142**, 2000, 149–156.
5. M. C. Britton. Publ. Astron. Soc. Pac., **118**, 2006, 885–900.
6. R. Villecroze, T. Fusco, B. Neichel, R. Bacon, and P. Y. Madec. In *3rd AO4ELT Conference*, Florence, 2013.
7. E. Masciadri and F. Lascaux. In *Proc. Soc. Photo-Opt. Instrum. Eng.*, **8447**, 2012.
8. R. W. Wilson. Mon. Not. R. Astron. Soc., **337**, 2002, 103–108.
9. T. Butterley, R. W. Wilson, and M. Sarazin. Mon. Not. R. Astron. Soc., **369**, 2006, 835–845.
10. R. Avila, J. Vernin, and E. Masciadri. Appl. Opt., **36**, 1997, 7898–7905.
11. A. Fuchs, M. Tallon, and J. Vernin. Publ. Astron. Soc. Pac., **110**, 1998, 86–91.
12. A. Tokovinin, V. Kornilov, N. Shatsky, and O. Voziakova. Mon. Not. R. Astron. Soc., **343**, 2003, 891–899.
13. N. Védrenne, V. Michau, C. Robert, and J. M. Conan. Opt. Lett., **32**, 2007, 2659–2661.
14. J. Voyez, C. Robert, J. M. Conan, L. Mugnier, E. Samain, and A. Ziad Opt. Express, in prep., 2013.
15. R. Conan. PhD thesis, Université de Nice-Sophia Antipolis, 2000.
16. A. Ziad, J. Borgnino, F. Martin, J. Maire, Y. Fanteï-Caujolle, R. Douet, E. Bondoux, and J. B. Daban. In *2nd AO4ELT Conference*, Victoria, 2011.
17. J. Osborn, R. Wilson, V. Dhillon, R. Avila, and H. Shepherd. In *3rd AO4ELT Conference*, Florence, 2013.
18. E. Masciadri, G. Rousset, T. Fusco, P. Bonifacio, J. Fuensalida, C. Robert, M. Sarazin, R. Wilson, and A. Ziad. In *3rd AO4ELT Conference*, Florence, 2013.
19. F. Vidal, E. Gendron, and G. Rousset. J. Opt. Soc. Am. A, **27**, 2010, 253–264.
20. A. Cortés, B. Neichel, A. Guesalaga, J. Osborn, F. Rigaut, and D. Guzman. Mon. Not. R. Astron. Soc., **427**, 2012, 2089–2099.